Application of a glutamate microsensor to brain tissue

Oldenziel, Weite Hendrik

Chapter 5

Evaluation of hydrogel-coated glutamate microsensors.

This chapter is based on the following paper:

Oldenziel WH, Dijkstra G, Cremers TIFH, Westerink BHC. Evaluation of hydrogel-coated glutamate microsensors. *Anal. Chem*. 2006, 78: 3366-78.

Abstract

Glutamate microsensors form a promising analytical tool for monitoring neuronally derived glutamate directly in the brain. However, when a microsensor is implanted in brain tissue, many factors can diminish its performance. Consequently, a thorough characterization and evaluation of a microsensor is required concerning all factors that may possibly be encountered in vivo. In this chapter the hydrogel-coated glutamate microsensor is thoroughly evaluated. Attention is paid to its selectivity, specificity, calibration, oxygen dependency, biofouling, operating potential dependency and linear range. In addition, successful microsensor experiments in microdialysate, in vitro (in organotypic hippocampal slice cultures) and in vivo (in anesthesized rats) are shown.

5.1 Introduction

It is hypothesized that a detection technique with an improved spatial and temporal resolution is required to detect neuronally derived glutamate in brain tissue. Several reports indicate that microsensors may fulfil these requirements, as they combine the selectivity of a biological recognition element (e.g. an enzyme) with the spatial and temporal resolution of voltammetry. However, although various studies exist which describe the construction and evaluation of different type of microsensors, the number of studies that report on microsensors being operated successfully *in vivo* or *in vitro* is rather limited (as discussed in chapter 1). Apparently, there are many reasons why microsensors can fail (Gregg and Heller, 1991a; Wisniewski et al., 2000a, b)

Although the hydrogel-coated glutamate microsensor has been successfully applied *in vivo*, information concerning its validation is scarce and limited to one study (i.e. Kulagina et al., 1999). In this chapter, the microsensor was thoroughly characterized and evaluated. Attention was given to its selectivity, specificity, calibration, oxygen dependency, biofouling, operating potential dependency and linear range. The microsensor was also investigated in microdialysate, *in vitro* (in organotypic hippocampal slice cultures) and *in vivo* (in the brain of anesthesized rats). In addition, an attempt was made to correlate the *in vivo* current output of the microsensor to extracellular glutamate concentrations.

5.2 Experimental section

Reagents

Glutamate oxidase (Glu-ox; G-0400; 6.5 units/mg) was purchased from USBiological (Swampscott, MA, USA). Horseradish Peroxidase type II (HRP; P-8250; 158 units/mg), ascorbate oxidase (AA-ox; A-0157; 133.4 Units/mg), [4-(2-hydroxyethyl)-1-piperazineethane-sulfonic acid] (HEPES), HEPES sodium salt, l-glutamate, l-ascorbic acid, l-glutamine and all other chemicals were obtained from Sigma (St. Louis, MO, USA). Poly(ethylene glycol) diglycidyl ether (PEGDGE), silver chloride and Nafion (5 % Nafion solution, 1100 equivalent weight) were obtained from Aldrich (Milwaukee, WI, USA). Acetone p.a., 2-propanol p.a. and D-glucose were obtained from Merck (Darmstadt, Germany). Gey's balanced salt solution (GBSS), Opti-MEM, 25% Hanks' balanced salt solution, 25% horse serum, serum-free Neurobasal medium and 2% B27 supplement were obtained from Gibco (Paisley, Scotland). $_{DL}$-TBOA was obtained from Tocris Bioscience (Bristol, UK). Artificial Cerebrospinal Fluid (aCSF), used for the calibration procedures, had the following composition: 145 mM Na^+, 1.2 mM Ca^{2+}, 2.7 mM K^+, 1.0 mM Mg^{2+}, 152 mM Cl- and 2.0 mM phosphate; pH 7.4 adjusted with sodium hydroxide. Salts were obtained from Merck (Darmstadt, Germany). The osmium redox-polymer (POs-EA) was synthesized by complexing poly (4-vinylpyridine) with $Os(bpy)_2Cl_2$-groups and partially quaternizing it with 2-bromoethylamine, as described in chapter 3. Solutions were made in ultra-purified water (U.P.; Elgastat maxima, Salm en Kipp). Some compounds were dissolved with the help of sonication and heating (e.g. uric acid). Enzymes solutions were made in HEPES buffer; the salt form of HEPES was added to a 10 mM solution of the acid form, until pH 8.

Construction and calibration of the microsensor

Carbon fiber electrodes (CFEs) were trimmed to a length of 200-500 µm and microsensors (glutamate- and background sensors) were constructed as reported in chapters 2 and 3. Microsensor studies were carried out by amperometrically operating the microsensor at a constant potential of – 150 mV versus an Ag/AgCl reference electrode [0.15 M NaCl]. Most studies were performed in a flow-injection analysis system (FIA). FIA-calibration of the microsensors was divided into a few steps, as described in chapter 3.

Interference is defined as the percentage of suppression of the original glutamate signal induced by addition of 200 µM AA. The suppression by different concentrations of AA, and of other reducing agents also has been investigated. Different flow rates were used for the study concerning the flow rate dependency, respectively 1.5, 1.25, 1.0, 0.75, 0.50, 0.25, 0.10 and 0.05 ml/min. The following glutamate concentrations were used to investigate the linear range of the microsensor: 10, 50, 100, 200, 300, 400, 500, 750 and 1000 µM. In several experiments the calibration of the microsensor was carried out in a beaker, i.e. in the studies concerning different types of calibration, microdialysate, and the dependency of hydrogen peroxide and oxygen. Compounds were added to a beaker containing aCSF, which was magnetically stirred and temperature controlled at 37 °C. A battery driven magnetic stirrer was used (Fischer Emergo BV, Landsmeer, The Netherlands) to avoid AC power-induced noise.

Animals and surgical procedures

Male albino rats of a Wistar-derived strain (275-320 gr.; Harlan, Zeist, The Netherlands) were used for the *in vivo* microsensor experiments and for collecting microdialysate. Rats were anesthetized with Equitensine (Bo et al., 2003), placed in a stereotaxic frame (Kopf, Tujunga, CA, USA), and kept unconscious with additional doses of Equitensine. The body temperature was monitored and maintained at 37°C with a homeothermic blanket (Temperature controller CMA 150; CMA, Solna, Sweden). Small holes were drilled in the skull for insertion of the microsensors (glutamate- and background) and the microinfusion pipet. Both microsensors were placed in close proximity in a V-shaped form at a distance of about 100 µm. The microsensors were implanted in the striatum at an angle of 25° at the following coordinates, AP: + 0.9, ML: - 0.1 and VD: - 7.1 mm from bregma point and dura respectively (Paxinos and Watson, 1986). A fused silica micropipette (75 µm i.d., 150 µm o.d.) was used for local drug delivery and was implanted at a distance of about 100 µm from the microsensors at the following coordinates AP: + 0.9, ML: + 3.0 and VD: - 6.0 mm. The Ag/AgCl reference electrode was coated with Nafion in a similar way as the microsensors (Moussy and Harrison, 1994) and was placed in the prefrontal cortex. Experiments were approved by the Animal Care Committee of the College of Mathematics and Natural Science of the University of Groningen.

Additional microsensor experiments were performed with dialysate, obtained from rats in separate microdialysis experiments. Microdialysis was performed with a home-made I-shaped cannula with a polyacrylonitrile / sodium methalyl sulfonate copolymer (ID: 0.22 mm; OD: 0.31 mm; AN 69, Hospal, Bologna, Italy) dialysis tubing (Santiago and Westerink, 1992). The dialysis probe was stereotactically implanted under the following conditions: isoflurane 2%, N_2O 300 ml/min, O_2 300 ml/min. Microdialysate was collected from rats that had been used 1 or 2 consecutive days before, i.e. 48-72 hrs after probe implantation. The probe was perfused with aCSF at a flow rate of 1.5 or 0.2 µl/min and the samples were collected on ice and protected from light. The microdialysate of several animals was pooled and stored at -80 °C. The microdialysate was collected mainly from the brain regions hippocampus and prefrontal cortex. Glutamate levels in microdialysate were determined by pre-column derivatization with o-phtaldialdehyde/ mercaptoethanol reagents, in combination with reversed-phase HPLC separation and fluoremetric detection (HPLC-FD) (Kehr, 1998). In the microdialysate experiments, the glutamate and background microsensor were placed in close proximity (< 100 µm) in a small volume vial (≈ 200 µl). The microdialysate was smoothly stirred and maintained at 37°C.

Experiments in organotypic hippocampal slice cultures

A series of microsensor experiments was performed in organotypic hippocampal brain slice cultures. Slice cultures were prepared according earlier described procedures (Noraberg et al., 1999) and were cultured between 2 to 5 weeks prior to their use in microsensor experiments. Experiments were performed by placing the insert with the slice culture in a petridish containing 1 ml of Neurobasal medium. The microsensors (glutamate and background) were implanted in close proximity (< 200 µm) within the slice culture and 200 µl of Neurobasal medium was placed on top of the slice culture to keep it moist. Drug solutions ($_{DL}$-TBOA 100 µM and KCl 100 mM) were prepared in Neurobasal medium and were administered by adding 4/5 part of the volume under the slice (in the petridish) and 1/5 on top of the slice. Consequently, no local differences in drug concentrations were induced and the drug had to mediate its effect via passive diffusion. Microsensors were used with a CFE length of 100 to 200 µm in order to deal with the thickness of the slice culture. It is important to note that experiments were regarded as a proof of principle of the performance of the microsensor in slice cultures. Accordingly, the precise localization of the microsensors

within the slice culture and the exact state of the viability of the slice culture was of secondary importance. Biofouling studies were also performed in the hippocampal slice cultures. The microsensors were placed in the slice cultures, removed at different time points for calibration in a FIA system, and carefully returned in the slice culture.

Oxygen dependency of the glutamate microsensor

The oxygen dependency of the glutamate microsensor was investigated as follows: a glutamate microsensor, an oxygen electrode, and a gas outlet were placed in a beaker containing 30 ml of aCSF, which was gently stirred and maintained at 37 °C. The dissolved oxygen levels (pO_2) in the aCSF were altered by purging with He or O_2. The exact pO_2 concentration (expressed in %) was determined with a polarographic Clark style electrode (YSI 5750; Yellow Springs Instruments, Ohio, USA), and the current output of the glutamate microsensor was monitored simultaneously. Prior to each experiment, the oxygen electrode was calibrated. This was performed under conditions similar to that under which the microsensor experiments were conducted in order to correct for parameters that may influence the dissolution of pO_2, e.g. temperature, pH, electrolyte composition, etc. Calibration was performed from 0 to 100% pO_2: 0 % reflected an oxygen free solution, which was induced by purging with helium (He; in order to remove most pO_2), followed by addition of sodiumdithionite, (which eliminated remnant pO_2). The condition of 100% oxygen saturation was induced by purging with pure oxygen until stabilization. Note: because experiments were performed in an open beaker (Fig. 4A-C), purging with He resulted in pO_2 levels of approximately 2%. This is similar to, or slightly lower than, the expected pO_2 levels in the brain. The oxygen dependency of the microsensor was also determined in a FIA system (Fig. 4D), in which the aCSF was either air or He saturated.

Expression of results and statistics

Experiments are presented as mean ± SEM. In several figures (Fig. 2, 3, 4, 7 and 8) the recordings of the microsensors were averaged and represented as a black line (mean) with a gray area (SEM). Sigmastat 3.0, was used to calculate statistics. Dependent on the type of study, data were analyzed either with a Mann-Whitney Rank Sum test (M-W Rank Sum test) or with One Way Anova followed by a Student-Newman-Keuls posthoc test. The latter was performed to analyze the *in vitro* and *in*

vivo results. For statistical analysis of the *in vitro* and *in vivo* results, the data (each second a data point) were averaged to minute sections and the minute prior to the treatment was compared to the post-treatment minutes. The linear range was investigated with linear regression with standardized residuals set at 2.0. In addition, the regression coefficient's and Pearson's coefficient's were calculated.

5.3 Results and Discussion

Calibration of the glutamate microsensor

When the microsensor is operated in brain tissue, its output is in current (pA) and calibration is required to translate these currents to glutamate concentrations. Two different types of calibration are generally applied: 1) Calibration in a beaker: the microsensors are positioned in a stirred beaker to which substrates are applied. In such an approach, steady-state conditions are established, i.e. the amount of substrate diffusing into the hydrogel equals the amount that is consumed by the enzymatic reaction. 2) Calibration in a flow injection analysis system (FIA): the microsensors are placed parallel in the flow of carrier solution (aCSF) and different concentrations of substrate are added to the flow at intermittent pulses. During FIA, steady state conditions do not occur, as the plug of substrate solution is replaced by pure aCSF before steady state conditions are reached. The slower the flow rate (or the longer the plug is applied), the closer the approach to the steady state current (Gorton et al., 1991; Elmgren et al., 1993).

An important question is which type of calibration better reflects the condition in the brain? While the presence of a constant glutamate concentration (non-neuronal and neuronal origin) is represented by steady-state conditions, fast transient glutamate waves (predominantly from neuronal origin) are represented by non-steady-state conditions. In this respect, the influence of the two types of calibration on the performance of the microsensor was investigated (Fig. 1). The microsensors were calibrated in a FIA system at different flow rates (Fig. 1A), as well as in a beaker (Fig. 1B). The sensitivity for glutamate was investigated for the following conditions: the sensitivity for glutamate itself, for glutamate in the presence of 200 µM AA, in the presence of 200 µM AA and 50 µM uric acid (UA), and in the presence of 400 µM AA and 100 µM UA. AA and UA were used because they profoundly reduced the performance of the microsensor, as will be discussed next (Table 1).

It was shown that the sensitivity for glutamate increased when the flow rate decreased. In addition, the sensitivity for glutamate at the lowest flow rates corresponded to that observed with calibration in a beaker. A high degree of interference was observed in the presence of AA and UA, especially at lower flow rates. A positive aspect of this interference was that the response of the microsensor became independent of the flow rate. It was also observed that the interference

induced by AA and UA was cumulative until a level of saturation, i.e. a further increment from 200 µM AA and 50 µM UA to 400 µM AA and 100 µM UA did not suppress the sensitivity much further. A typical example of a microsensor response to 10 µM glutamate was presented in Fig. $1C_1$. It was observed that both the peak height and the area under the curve (AUC) were increased when the flow rate decreased. Differences in response kinetics of the microsensor were also visible.

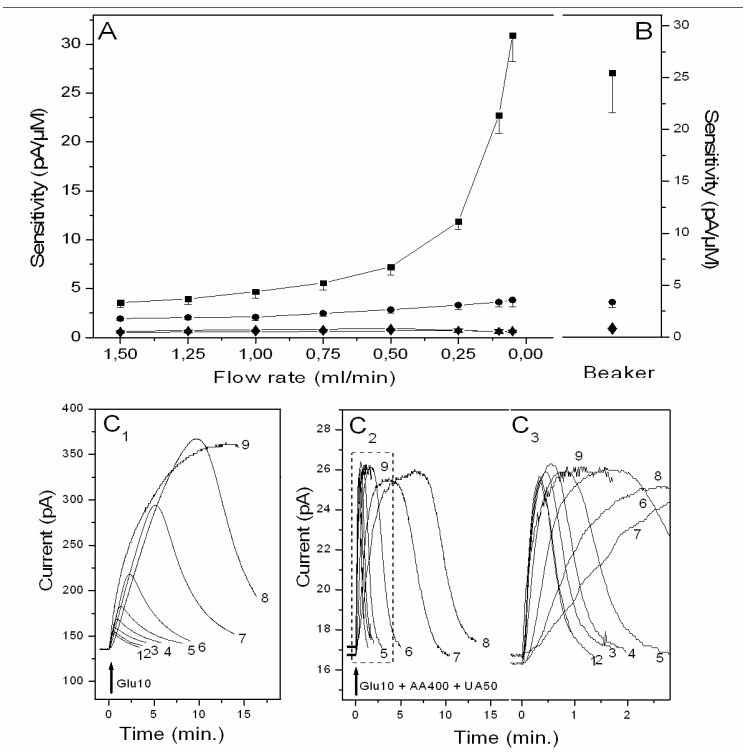

Figure 1: Calibration of the glutamate microsensor. ***A)*** *Calibration in a FIA system at different flow rates. Calibration was performed at the following conditions: -■- = glutamate (n = 11); -●- = glutamate + AA 200 µM (n = 9); -▲- = glutamate + AA 200 µM + UA 50 µM (n = 8); -▼- = glutamate + AA 400 µM + UA 100 µM (n = 8).* ***B)*** *Calibration in a beaker at the same conditions as presented in* ***(A)*** *(respectively, n = 64, 19, 13 and 15). Note, the significant decrease in sensitivity in the presence of AA and UA was not marked (p < 0.05; M-W Rank sum test)* ***C_1)*** *A typical example of a microsensor response to glutamate 10 µM. Nrs. 1 to 8 indicate the flow rate at which the FIA calibration was performed (respectively 1 = 1.5, 2 = 1.25, 3 = 1.0, 4 = 0.75, 5 = 0.5, 6 = 0.25, 7 = 0.10 and 8 = 0.05 ml/min), nr. 9 indicates calibration in a beaker.* ***C_2)*** *Same as* ***(C_1)*** *but now glutamate 10 µM was administered in the presence of AA 400 µM and UA 100 µM. The first part of graph C_2 is outlined and visualized in Fig.* ***C_3****.*

An example of a microsensor response to 10 µM glutamate in the presence of 400 µM AA and 100 µM UA was presented in Fig. $1C_2$ (a magnification of Fig.$1C_2$ was presented in Fig.$1C_3$). It was shown that the response to glutamate and the suppression by the reducing agents had reached an equilibrium, which resulted in a plateau value at lower flow rates. Interestingly, in the presence of reducing agents much faster response times were observed (down to approximately 9 seconds).

It is concluded that both type of calibrations produce similar results when the microsensor is calibrated in the presence of reducing agents. In the next paragraphs FIA calibration at 1 ml/min was applied as a standard calibration. However, some studies required calibration in a beaker (i.e. the studies concerning microdialysate, hydrogen peroxide and oxygen dependency), as will be indicated.

Selectivity and specificity of the glutamate microsensor

Specificity and selectivity are important properties of a microsensor. In the brain many electrochemically active compounds are present that can interfere with the performance of the glutamate microsensor at different levels: A) Immediate oxidation or reduction of compounds at the CFE surface, B) Interference within the redox cascade of the hydrogel, and C) Substrate aspecificity of Glu-ox.

A. Electrochemical reaction at the CFE surface

Any compound that is electrochemically active at the applied potential will contribute to the current output of the microsensor. To reduce this type of interference, the application of an optimal operating potential is of crucial importance. First, the influence of the operating potential on the response to glutamate was investigated (Fig. 2A). The experiments were conducted by calibrating the microsensor in a FIA system at different operating potentials. It was observed that between -250 and 250 mV the output of the microsensor was stable. When the potential was decreased below -250 mV, the output for glutamate remained similar, but a large basal reduction current started to occur, which was probably due to reduction of O_2 at the CFE. When the potential was increased above 250 mV, the sensitivity for glutamate decreased, likely due to a decrease in Os^{2+}. In addition, the noise level of the microsensor increased dramatically and both a basal oxidation current and side reactions started to occur, probably due to immediate oxidation of H_2O_2 at the CFE surface and due to short-circuiting of Glu-ox to Os^{3+}.

At low operating potentials, easily oxidizable compounds, for example dihydroxyphenylacetic acid (DOPAC), uric acid (UA), and especially AA, might interfere with the microsensor. AA was used as a representative of these easily oxidizable compounds due to its low oxidation potential and its high concentration within the brain. Bolus injections of 200 µM AA were administered to sensors with and without AA-ox (Fig. 2B). It was observed that significant oxidation of AA started at -100 mV and increased strongly with increasing operating potentials at sensors without AA-ox, whereas the response of sensors with AA-ox was minimal. This implies that AA-ox is very effective in scavenging AA, as discussed previously (chapter 3). Reduction of O_2 started at both sensors at potentials lower than –250 mV (results not shown). It is concluded that a potential of -150 mV is the optimal operating potential.

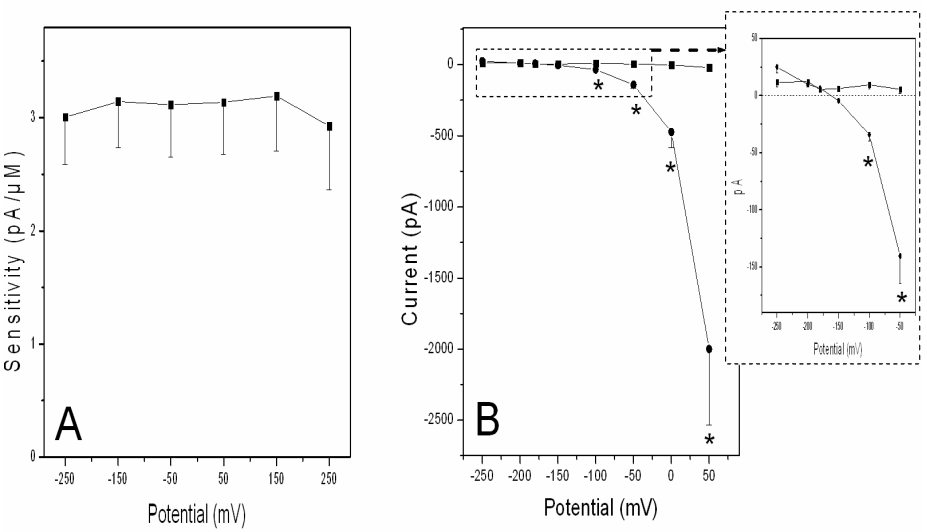

Figure 2: Influence of the operating potential on the performance of the glutamate microsensor. ***A)*** *Sensitivity for glutamate at different operating potentials (n = 10).* ***B)*** *Bolus injections of AA 200 µM at different operating potentials to glutamate microsensors with (-■-; n = 8) and without (-●- ; n = 12) AA-ox incorporated into the hydrogel. All operating potentials were applied versus an Ag/AgCl [0.015 M NaCl] reference electrode. The calibrations were performed in a FIA system. * Denotes a statistically significant difference compared to AA-ox containing microsensors. (p < 0.05; M-W Rank sum test).*

B. Interference within the redox cascade

Electrochemically active compounds can also affect the performance of the microsensor by interfering at different levels in the redox-cascade of the hydrogel. Therefore, the influence of different electrochemically active compounds was investigated (Table 1). At first, glutamate was injected to microsensors in a FIA system, followed by glutamate spiked with the compound under investigation, and finally the compound itself was injected. A glutamate concentration of 100 µM was chosen, as extracellular glutamate concentrations in the brain were reported to reach these levels under certain conditions (Kulagina et al., 1999; Danbolt, 2001).

In Table 1 it is shown that the microsensor is rather selective in detecting glutamate. AA, despite incorporation of AA-ox within the hydrogel, and UA appeared to decrease the sensitivity of the microsensor most strongly. Both compounds are strong reducing agents and are negatively charged, which favour their diffusion within the hydrogel by attraction to the positively charged POs-EA (Chen et al., 2000). AA and UA interfereby reducing the intermediate steps in the redox cascade that are present in an oxidized state (Os^{3+}, HRP_{ox} and H_2O_2). Dopamine, noradrenaline and cysteine induced only small effects. Interaction with the catalytic activity of POs-EA was most likely responsible for these effects. However, it could not be fully excluded that injection artifacts also contributed to the response. For example, small changes in pH and electrolyte composition also induced injection artifacts (results not shown). The larger effect of DOPAC was contributed both to an interaction with POs-EA and to an immediate effect on the CFE surface (Ni et al., 1999; Mikeladze et al., 2002). Importantly, the responses of DOPAC, dopamine, noradrenaline and cysteine were also seen at the background microsensor (results not shown). The microsensor also displayed a high sensitivity for hydrogen peroxide, which will be discussed in detail below.

AA is present in high concentrations in the brain (100-500 µM) and large and rapid fluctuations in its extracellular concentration can occur that also might be related to glutamergic activity (Grünewald, 1993; Yusa, 2001). In this respect, the influence of AA on the microsensor response was investigated in more detail (Fig. 3). At first, the influence of different concentrations AA (range 0 to 500 µM) on the sensitivity of the microsensor for glutamate was investigated (Fig. 3A). It was observed that an increasing concentration of AA caused a gradual decrease in sensitivity, in which an

Treatment[a]	n	Relative response to the the glutamate signal	Treatment[a]	n	Relative response to the the glutamate signal
glutamate 100 µM (= glu 100)		1			
Neurotransmitters			***Reducing agents***		
glu 100 + adrenaline 5 µM	6	0.93 ± 0.08 (n.s.)	glu 100 + acetylcysteine 5 µM	7	0.98 ± 0.14 (n.s.)
adrenaline 5 µM		0	acetylcysteine 5		0
glu 100 + aspartate 100 µM	10	1.03 ± 0.09 (n.s.)	glu 100 + alfatocopherol 5 µM	4	1
aspartate 100 µM		0.03 ± 0.03 (n.s.)	alfatocopherol 5		0
glu 100 + dopamine 5 µM	9	0.98 ± 0.06 (n.s.)	glu 100 + ascorbic acid 200 µM	19	0,78 ± 0.05 *
dopamine 5 µM		0.12 ± 0.07 *	ascorbic acid 200 µM		0.03 ± 0.03 (n.s.)
glu 100 + GABA 5 µM	4	1	glu 100 + ascorbic acid 500 µM	19	0,62 ± 0.11 *
GABA 5 µM		0	ascorbic acid 500 µM		0.05 ± 0.04 (n.s.)
glu 100 + glycine 10 µM	4	1	glu 100 + cysteine 5 µM	8	1.08 ± 0.11 *
glycine 10 µM		0	cysteine 5 µM		0.18 ± 0.10 *
glu 100 + 5-HT 1 µM	8	1.05 ± 0.03 *	glu 100 + glutathione $_{red}$ 5 µM	7	1
5-HT 1 µM		0	glutathione $_{red}$ 5 µM		0
glu 100 + noradrenaline 5 µM	10	0.97 ± 0.06 (n.s.)	glu 100 + glutathione $_{red}$ 50 µM	7	0.94 ± 0.03 *
noradrenaline 5 µM		0.07 ± 0.04 *	glutathione $_{red}$ 50 µM		0
			glu 100 + $NADH_2$ 5 µM	4	1
Neurotransmitter metabolites			$NADH_2$ 5 µM		0
glu 100 + α–ketoglutarate 100 µM	4	1	glu 100 + $NADH_2$ 50 µM	7	0.86 ± 0.07 *
α–ketoglutarate 100 µM		0	$NADH_2$ 50 µM		0
glu 100 + DOPAC 20 µM	9	0.90 ± 0.3 *	glu 100 + NADH 5 µM	4	1
DOPAC 20 µM		0.56 ± 0.3 *	NADH 5 µM		0
glu 100 + glutamine 100 µM	10	1.0 ± 0.05 (n.s.)	glu 100 + NADH 50 µM	7	0.95 ± 0.09 *
glutamine 100 µM		0.06 ± 0.02 *	NADH 50		0
glu 100 + glutamine 500 µM	4	0.96 ± 0.08 (n.s.)	glu 100 + pyruvate 10 µM	4	1
glutamine 500 µM		0.07 ± 0.06 *	pyruvate 10 µM		0
glu 100 + 5-HIAA 10 µM	8	0.97 ± 0.08 (n.s.)	glu 100 + uric acid 50 µM	14	0.72 ± 0.27 *
5-HIAA 10 µM		0	uric acid 50 µM		0
glu 100+ histidine 100 µM	5	1	glu 100 + uric acid 100 µM	31	0.67 ± 0.12 *
histidine 100 µM		0	uric acid 100 µM		0
glu 100 + HMPG 10 µM	4	1			
HMPG 10 µM		0	***Other***		
glu 100 + HVA 20 µM	6	1	glu 100 + d-glutamate 100 µM	7	1
HVA 20 µM		0	d-glutamate 100 µM		0
glu 100 + tyrosine 10 µM	7	0.97 ± 0.05 (n.s.)	glu 100 + glucose 100 µM	4	1
tyrosine 10 µM		0	glucose 100 µM		0
glu 100 + tryptophane 10 µM	4	1	glu 100 + lactate 100 µM	4	1
tryptophane 10 µM		0	lactate 100 µM		0
			glu 100 + H_2O_2 1 µM	9	7,16 ± 3,55 *
			H2O2 (sensitivity)		17.9 ± 8.9 * (pA/µM)

*Table 1: Influence of different electrochemically active compounds on the performance of the glutamate microsensor. Investigated was the effect of the interferent itself and when coinjected to glutamate 100 µM (set as 1) in a FIA system. * Denotes a statistically significant difference (p < 0.05; M-W Rank sum test). n.s.: non-significant.* [a] *Abbreviations: DOPAC: 3,4-dihydroxyphenylacetic acid, GABA: γ–aminobutyric acid, 5-HIAA: 5-hydroxy-indole-3-acetic acid, HMPG: 4-hydroxy-3-methoxy-phenylglycol, 5-HT: serotonin, HVA: 4-hydroxy-3-methoxy-phenylacetic acid, NADH: β-nicotinamide adenine dinucleotide, reduced form, $NADH_2$: β-nicotinamide adenine dinucleotide, reduced form.*

increase of AA from 0 to 500 µM decreased the sensitivity approximately 40 %. When AA was increased from 100 to 500 µM, which represents a broad physiological response, the sensitivity of the microsensor decreased approximately 25%. The response of the microsensor to different concentrations of glutamate (range from 5 to 100 µM) in the presence of 200 µM AA was also investigated (Fig. 3B). It was observed that the extent of interference did not change when glutamate concentrations were altered. It is possible that the passive diffusion of glutamate and AA is in equilibrium with the quantity of intermediate steps that are induced to an oxidized state in the redox cascade.

From these observations it is concluded that the microsensor is capable of detecting dynamic changes of glutamate in the presence of high concentrations of AA, and that strong fluctuating levels of AA only affect the microsensor moderately.

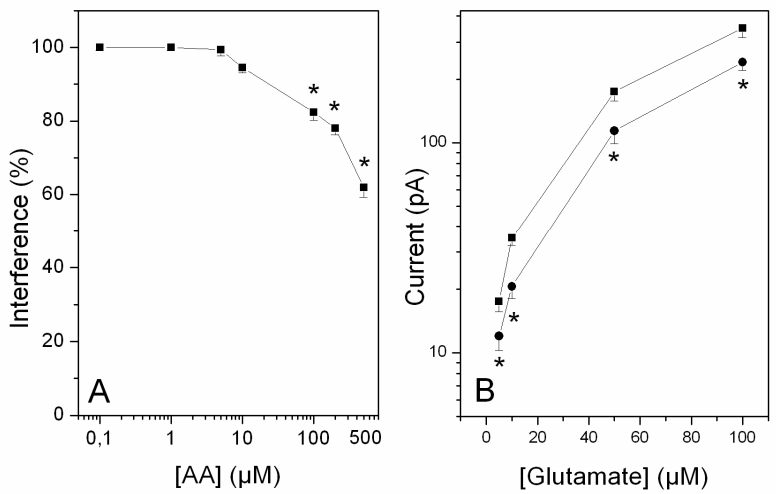

Figure 3: Influence of AA on the performance of the glutamate microsensor. ***A)*** *Influence of different concentrations of AA on the glutamate response of the microsensor. The concentration AA coinjected to glutamate 100 µM was varied from 0.01 to 500 µM (n = 19). The sensitivity for glutamate 100 µM, without coinjecting AA, was set as 100 %. * Denotes a statistically significant difference compared to the control values (p < 0.05; One-Way ANOVA followed by a Dunn's post-hoc test).* ***B)*** *The influence of AA 200 µM on different concentrations of glutamate (5, 10, 50 and 100 µM). Response of the microsensor (n = 11) to: -■- = glutamate, -●- = glutamate in the presence of AA 200 µM. * Denotes a statistically significant difference compared to the glutamate values. (p < 0.05; M-W Rank sum test). Both experiments were performed in a FIA system.*

C. Substrate specificity of Glu-ox

When microsensor experiments are performed *in vitro* or *in vivo*, both a glutamate and background microsensor are used. The difference between both microsensors is the signal detected by Glu-ox. This implies that all the non-specific signals mentioned in A) and B) are also detected by the background microsensor and that the substrate specificity of Glu-ox is important. Glu-ox has been reported to be a very selective enzyme, displaying only a slight sensitivity for l-aspartate (0.6 %), glutamine (0.08 %), and for the, non-physiological, neurotoxin β-N-oxalyl-α,β-diamino-propionic acid (β-ODAP) (Kusakabe et al., 1983; Belay et al., 1997; Mikeladze et al., 2002). It was shown that the microsensor displayed a slight sensitivity for glutamine (Table 1). However, this sensitivity disappeared completely in the presence of glutamate and AA (results not shown).

Performance of the microsensor in microdialysate

Although many different electrochemical active compounds have been investigated in Table 1, it is impossible to each individual compound present in the brain. For that reason the performance of the microsensor was investigated in microdialysate (Fig. 4), as microdialysate contains all molecular compounds present in the extracellular fluid (ECF) which are < 6 kDa (molecular weight cut-off of the dialysis membrane). The concentration of the different compounds within microdialysate is a function of the mass transport of the compound through the brain, the membrane properties, and the dialysis perfusion fluid (Benveniste and Hüttemeier, 1990; Stenken, 1999). The performance of the glutamate microsensor was investigated in two types of microdialysate: microdialysate collected at 1.5 µl/min (Fig. 4A), which results in a concentration recovery of 15 to 30 %, and microdialysate collected at 0.2 µl/min (Fig. 4B), which results in a recovery close to 100 %. The response of both the glutamate and background microsensor was investigated by placing the two sensors in close proximity (< 100 µm) in a small volume vial (≈ 200 µl), which was slowly stirred and temperature controlled at 37°C. The difference between both microsensors indicated the basal glutamate concentration present in the microdialysate, which was quantitated with HPLC-FD at respectively 2.7 (Fig. 4A) and 6.1 µM (Fig. 4B). Next, the microdialysate was spiked with a glutamate concentration of 10 µM to investigate whether the microsensor was capable of selectively responding to glutamate changes under these conditions. It was observed that the microsensors behaved very

differently in the two types of microdialysate. The high recovery microdialysate (Fig. 4B) resulted in a higher concentration of glutamate, but likely also in a higher concentration of reducing agents. This caused a lower response to glutamate, a lower background current of both microsensors, a lower variation in detected current, and faster microsensor kinetics, e.g. the response time decreased from about 110 seconds (Fig. 4A) to about 8 seconds (Fig. 4B). In addition, in the high recovery microdialysate the microsensor responded in a linear way both to the basal glutamate concentration (6.1 µM), as to dynamic glutamate changes (added 10 µM), in contrast to its performance in the low recovery microdialysate. This discrepancy is explained by the variation in basal current output of the microsensors.

With amperometric recordings, each microsensor induces a basal current output. Several aspects determine this current, for example the operating potential, the environment in which the sensor is applied, pO_2 levels and, in particular, the thickness of the hydrogel layer.

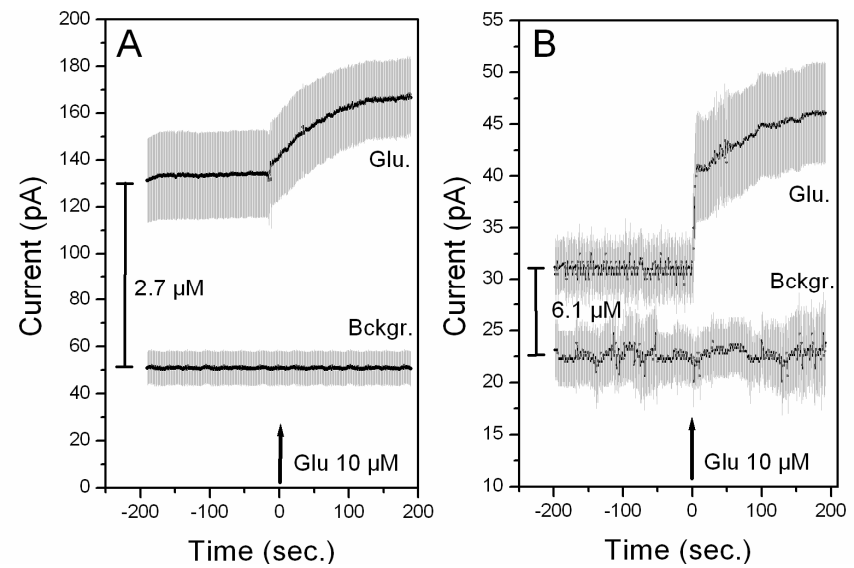

Figure 4: Performance of the microsensors in microdialysate. ***A)*** *Response of glutamate (Glu. ; n = 9) and background microsensors (Bckgr.; n = 6) to microdialysate collected at a flow rate of 1.5 µl/min, which contained a basal glutamate concentration of 2.7 µM, and to an additional glutamate 10 µM administration.* ***B)*** *Same as* ***(A)*** *but now the experiments were carried out in microdialysate collected at a flow rate of 0.2 µl/min, which contained a basal glutamate concentration of 6.1 µM (Glu., n = 8; Bckgr., n = 6).*

When reducing agents are not present, or only at low concentrations, the basal current output of the sensor is not restricted and contributes significantly to the detected signal. This obscures the glutamate detection properties. On the contrary, in the presence of high concentrations of reducing agents this basal current output is strongly suppressed, which improves the interpretation of the glutamate signal.

Interestingly, the performance of the microsensor in concentrated microdialysate, in terms of sensitivity, interference, basal current and response time, was comparable with the performance in the presence of high concentrations of AA and UA (see Fig. 1). Therefore, high concentrations of AA and UA can be used as a substitute for concentrated microdialysate within calibration studies.

It is concluded that, although physiological concentrations of reducing agents strongly decreased the sensitivity of the microsensor, the microsensor is still capable of monitoring dynamic glutamate levels within microdialysate.

Influence of hydrogen peroxide on the performance of the microsensor

There is increasing evidence that hydrogen peroxide (H_2O_2) plays an important role as a diffusible neuromodulator within the brain and that glutamate might be involved in this mechanism (Avshalumov, 2003; Kulagina and Michael, 2003). Because H_2O_2 is an intermediate step in the redox-cascade of the hydrogel, the microsensor displayed a high sensitivity for H_2O_2 (Table 1). In this respect, it is of interest to further investigate the possible influence of H_2O_2 on the performance of the microsensors (Fig. 5). The glutamate and background microsensor were placed in close proximity (< 100 µm) in a small volume vial (≈ 200 µl; which was slowly stirred and controlled at 37°C). At first, a glutamate concentration of 10 µM was administered in duplicate. It was shown that only the glutamate microsensor responded and that leakage of H_2O_2 outside the hydrogel was not observed, in contrast to other type of biosensors (e.g. Burmeister et al., 2002). Next, increasing concentrations of H_2O_2 were administered. It was shown that the microsensor displayed a high sensitivity for H_2O_2. More importantly, both the glutamate and background microsensor responded identically to the different H_2O_2 concentrations.

It is concluded that the background microsensor can be used as an appropriate reference sensor to correct for possible H_2O_2 effects.

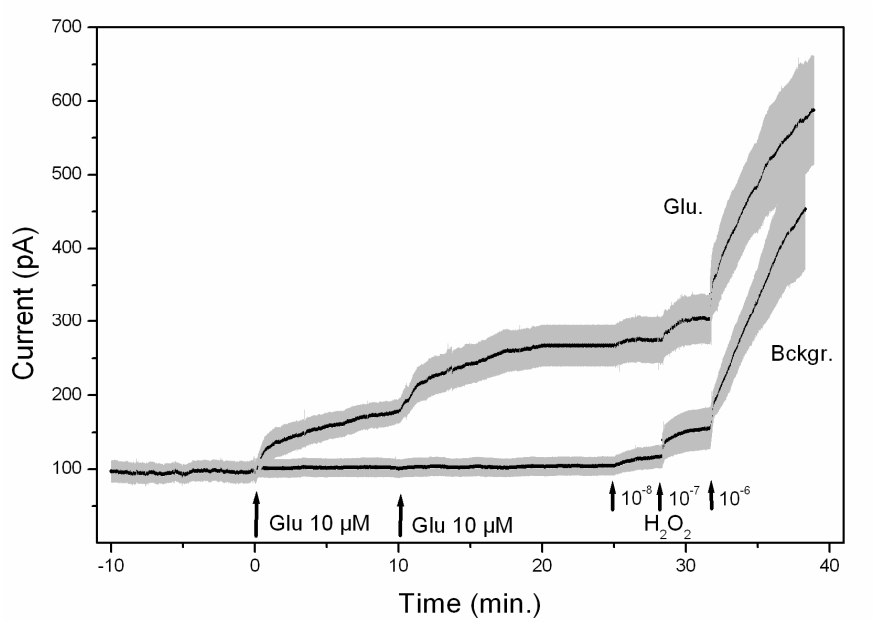

Figure 5: Influence of hydrogen peroxide on the performance of the microsensors. Glutamate 10 µM was administered in duplicate, followed by H_2O_2 concentrations of 10 nM (10^{-8}), 100 nM (10^{-7}) and 1 µM (10^{-6}). The response of both glutamate (Glu.; n = 5) and background microsensors (Bckgr.; n = 5) was monitored.

Oxygen dependency of the microsensor

As both Glu-ox and AA-ox utilize oxygen (O_2) as a co-substrate, it is necessary to investigate the exact oxygen dependency of the glutamate microsensor (Fig. 6). Dissolved oxygen levels (pO_2) in the brain of anesthesized rats (detected with microelectrodes with comparable dimensions as the glutamate microsensor) are between 15 and 40 mm Hg. This corresponds to 2-5 % of dissolved oxygen, and depends on the brain region, neuronal activity and local blood flow. In awake animals these levels are slightly higher (Hu and Wilson, 1997; Masomoto et al., 2003).

The oxygen dependency of the glutamate microsensor was investigated for two conditions: the oxygen dependency in the presence of glutamate (Fig. 6A), and in the presence of both glutamate and AA (Fig. 6B). To investigate the oxygen consumption of Glu-ox (Fig. 6A), the glutamate microsensor was placed in a small volume beaker (which was slowly stirred and controlled at 37°C) and a glutamate

concentration of 10 µM was administered. Next, the pO_2 levels were varied. It was shown that the glutamate signal was barely affected by the altered pO_2 levels and that the sensitivity for glutamate decreased approximately 9 % when the pO_2 levels were decreased from 21 % to 2 %. In a following step, 200 µM AA was administered (not indicated) prior to a second application of glutamate (Fig. 6B). Now, both oxygen consuming enzymes were active. It was shown that the output of the microsensor was profoundly affected by the pO_2 levels, and changes of approximately 60 % were observed when oxygen levels were varied from 21 % to respectively 2 % and 100 %. Interpretation of the results of both Fig. 6A and B was obscured by the fact that changes in pO_2 levels also affected the basal current output of the glutamate microsensor, as shown in Fig. 6C. This is most likely explained by a direct reduction of O_2 at the CFE, but maybe a catalytic reaction of O_2 with POs-EA also contributed. It is clear that the relative contribution of this effect is much larger in Fig. 6B than in Fig. 6A, based on the smaller absolute current output. When the results of Fig. 6A and B were corrected for these basal effects, the glutamate signals displayed a decline of respectively 8.5 and 26 %, when the oxygen levels were decreased from 21 % to 2%.

To eliminate these basal effects, the oxygen dependency was also investigated in a FIA system (Fig. 6D). The glutamate microsensors were calibrated with glutamate, eventually in combination with 200 µM AA, in a flow of aCSF (1 ml/min) containing 21 or 2 % pO_2. Decreasing the pO_2 levels from 21 to 2 % suppressed the sensitivity for glutamate approximately 8 %, while the sensitivity in the presence of AA was suppressed approximately 17 %. Both values were consistent with the results of Fig. 6A and B, when corrected for the basal oxygen effects.

The higher oxygen dependency in the presence of AA is explained by the fact that, beside both oxygen consuming enzymes being active, the concentration of AA-ox within the hydrogel is much higher than Glu-ox. In addition, when the activity of AA-ox is limited by oxygen deprivation, less AA will be scavenged, and in turn a larger suppression of the glutamate signal occurs due to interference by AA in the redox cascade.

It is concluded that pO_2 levels that are normally present in the brain most likely will limit the sensitivity of the microsensor only to a small extent. In addition, physiological fluctuations of pO_2 (in the range 2 to 7 %) probably will not influence the response of the microsensor largely.

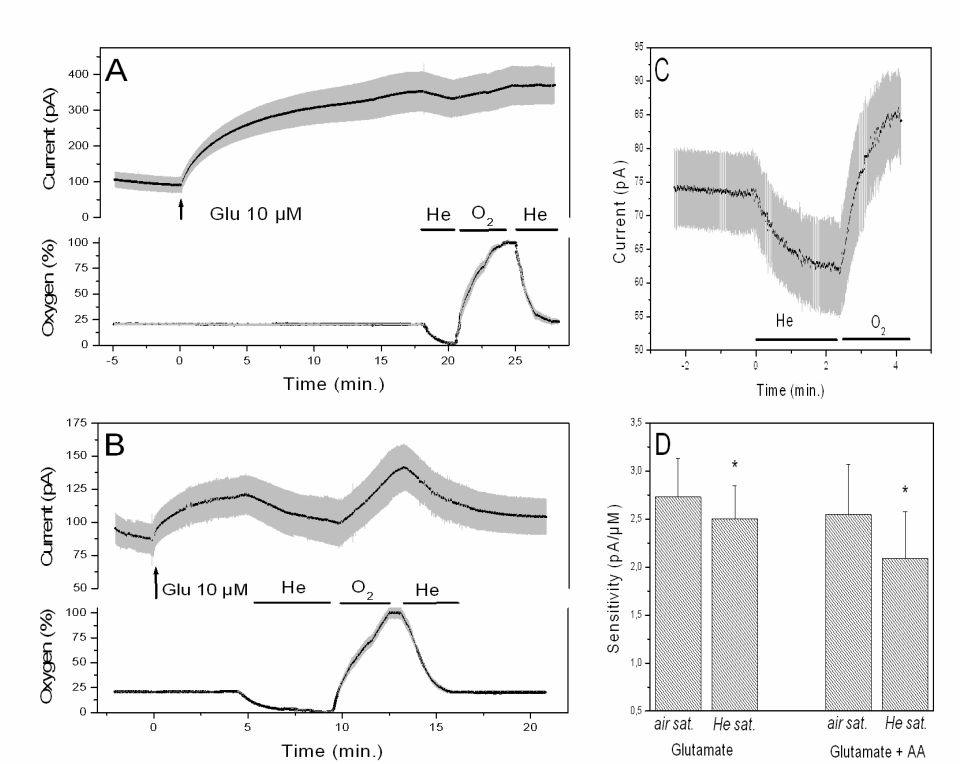

Figure 6: Determination of the oxygen dependency of the glutamate microsensor. ***A)*** *Response of the microsensor to a 10 µM glutamate concentration at different dissolved oxygen levels (n = 11) in a beaker. Upper trace: current output of the glutamate microsensor. Lower trace: dissolved oxygen levels monitored with an oxygen electrode and expressed in %.* ***B)*** *Same as* ***(A)*** *but now 200 µM AA was added prior to a second glutamate administration (n = 11).* ***C)*** *Changes in the basal current of the glutamate microsensor as a result of changes in dissolved oxygen levels (n = 10).* ***D)*** *Oxygen dependency of the glutamate microsensor determined in a FIA system (n = 12). Left: sensitivity for glutamate at air and He saturated conditions. Right: same as left, but now the sensitivity for glutamate was determined in the presence of 200 µM AA. * Denotes a statistically significant difference (p < 0.05; M-W Rank sum test; when air saturated values set as 100%).*

Influence of biofouling on the performance of the microsensor

Biofouling is a major cause of microsensor failure during *in vivo* experiments. Biofouling is regarded as the deterioration of the performance of the microsensor by accumulation of proteins, cells and other biological materials to the surface of the microsensor. Other possible biocompatibility based failures are microsensor

passivation, fibrous encapsulation and biodegradation (Wisniewski et al., 2000; Wisniewski and Reichert, 2000). Therefore, the influence of biofouling on the microsensor performance was investigated (Fig. 7). The glutamate microsensor was calibrated in a FIA system and the sensitivity for glutamate before and after an *in vivo* experiment, which lasted approximately 3 hours, was compared (Fig. 7A). Note, the sensors were immediately calibrated after the *in vivo* experiment to obtain an accurate indication of the biofouling (Wilson and Gifford, 2005).

Two conditions were investigated: the sensitivity for glutamate and for glutamate in the presence of 200 µM AA. The sensitivity for glutamate decreased approximately 40 %, while the sensitivity for glutamate in the presence of AA declined approximately 48 %. This indicated that the diffusion of both glutamate and AA was about equally limited due to biofouling. An additional advantage was that biofouling also decreased the oxygen dependency of the microsensors, i.e. in Fig. 6 it was shown that the sensitivity of the microsensor for glutamate in the presence of AA declined approximately 17 % when pO_2 levels were decreased from 21 to 2 %. Biofouled microsensors only displayed a 12 % decrease under these conditions (results not shown). It is possible that biofouling selectively impairs the diffusion of the much larger glutamate and AA into the hydrogel compared to the smaller O_2. In this respect, biofouling also influenced the linear range of the microsensor, as discussed below.

An important question is how the decline in microsensor sensitivity due to biofouling occurs. This was not possible to investigate in detail in a living animal. Therefore, experiments were performed in the best possible alternative: organotypic brain slice cultures. A recent publication has demonstrated that brain slice cultures are a viable alternative to investigate biofouling, as both neurons and glia are present in a native three-dimensional state (Koeneman et al., 2004). The decrease in microsensor sensitivity over time as a result of biofouling was investigated for four conditions: the decrease in sensitivity for glutamate and for glutamate in the presence of 200 µM AA, for microsensors with (Fig. 7B) and without (Fig. 7C) a Nafion layer. The experiments were performed by placing a microsensor in organotypic hippocampal slice cultures, removing it at different time points for FIA calibration and carefully returning it in the slice culture. It was shown that the sensitivity declined within the first hour after implantation, while the next 24 hrs the sensitivity remained stable. During the following 24 hrs the sensitivity declined again. It is not known

whether the observed results were solely due to biofouling, or whether other factors also contributed, as it was difficult to maintain all experimental conditions stable during 48 hrs. It was shown that the microsensors with a Nafion layer displayed less decline in sensitivity than the sensors without a Nafion layer, indicating its beneficial role in the prevention to biofouling. Again, it was shown that the sensitivity for glutamate and for glutamate in the presence of AA decreased in a similar fashion. Because the sensitivity of the microsensors declined only during the first hour of implantation, it is concluded that after an initial stabilization period the *in vitro* and *in vivo* results can be interpreted without considering a gradual decrease in the sensitivity of the microsensor.

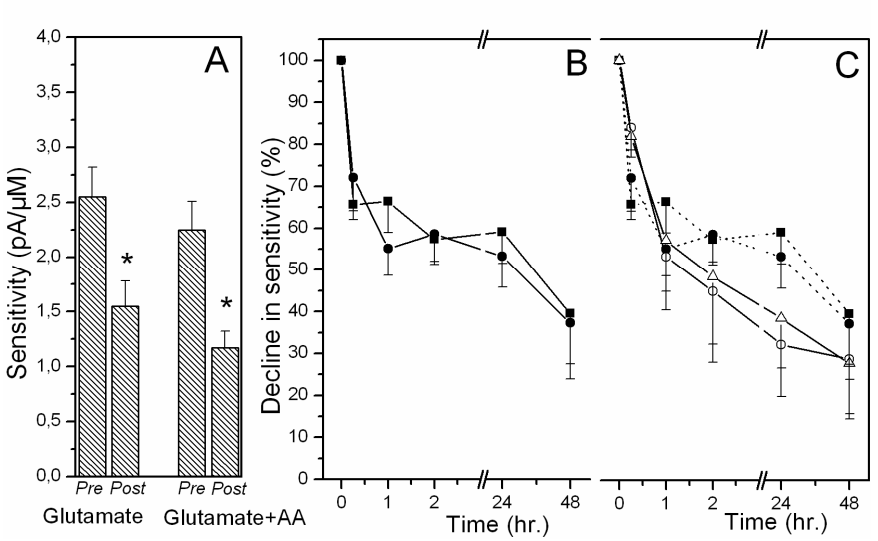

Figure 7: Influence of biofouling on the performance of the glutamate microsensor. ***A)*** *Sensitivity of the microsensor, determined in a FIA system, before (Pre) and after (Post) an in vivo experiment (n = 9). Left, sensitivity for glutamate. Right: the sensitivity for glutamate in the presence of AA 200 µM. * Denotes a statistically significant difference (p < 0.05; M-W Rank sum test).* ***B)*** *Decline of the sensitivity of the microsensor because of biofouling. The microsensors were calibrated at the following time points: t = 0 (precalibration), t = 15 min, t = 1 hr, t = 2 hr, t = 24 hr. and t = 48 hr. Investigated were the sensitivity for glutamate (-■-) and for glutamate in the presence of 200 µM AA (-●-) (n = 8). Note, the sensitivity was significantly decreased at all investigated time points compared to t = 0 (p < 0.05; M-W Rank sum test; not indicated).* ***C)*** *The influence of a Nafion coating on the decline in sensitivity. Microsensors without a Nafion coating (-○- = sensitivity for glutamate, -Δ- = sensitivity for glutamate in the presence of 200 µM AA (n = 11)) were compared with microsensors with a Nafion coating. The latter (results of* ***B)*** *were presented as dashed lines.*

Linear range of the microsensor

The brain contains large amounts of glutamate, of which only a minor fraction is present extracellular. Although the exact extracellular concentration is still a matter of debate, it is known that glutamate concentrations reach peak mM concentrations within the synaptic cleft (Bergles et al., 1999; Danbolt, 2001). In this respect it is important that the glutamate microsensor is capable of detecting extracellular glutamate concentrations over a wide linear range. The linear range of the glutamate microsensor was investigated in a FIA system for two conditions: for glutamate (Fig. 8A) and for glutamate at conditions mimicking the *in vivo* situation most closely (Fig. 8B). Throughout this study it appeared that conditions which resembled the *in vivo* situation most closely were: post *in vivo* calibration of a biofouled microsensor, at oxygen deprived conditions (≈ 2% pO_2), and in the presence of high concentrations of AA (200 µM) and UA (50 µM). It was observed that the sensitivity of the microsensor at these conditions decreased from 2.57 ± 0.28 to 0.55 ± 0.07 pA/µM (n = 12). In addition, the response time of the microsensor decreased to approximately 8 seconds. In Fig. 8A it was shown that the microsensors displayed linearity for glutamate up to 500 - 750 µM. The regression coefficient's (R^2) from 10 to 1000, 10 to 750 and 10 to 500 µM were respectively: 0.956 ± 0.011, 0.972 ± 0.007 and 0.989 ± 0.004 (with a Pearson's coefficient < 0.001). Most likely the linear range of the sensor under these conditions was controlled by the thickness of the hydrogel layer. Although conditions mimicking the *in vivo* situation decreased the sensitivity of the microsensor significantly, its linear range was not altered (Fig. 8B). The R^2s from 10 to 1000, 10 to 750 and 10 to 500 µM were respectively: 0.963 ± 0.016, 0.971 ± 0.016 and 0.978 ± 0.014 (Pearson's coefficient < 0.001). It is likely that several mechanisms are in equilibrium: on one hand a limitation of the microsensor response to glutamate by interference and oxygen deprivation, while on the other hand a restriction in the diffusion of glutamate into the hydrogel by biofouling. The latter will increase the (apparent) K_m of the microsensor (Garguilo et al., 1993; Kenausis et al., 1997). It is concluded that the linear range of the microsensor is probably sufficient for the concentrations of glutamate that will be encountered *in vivo*.

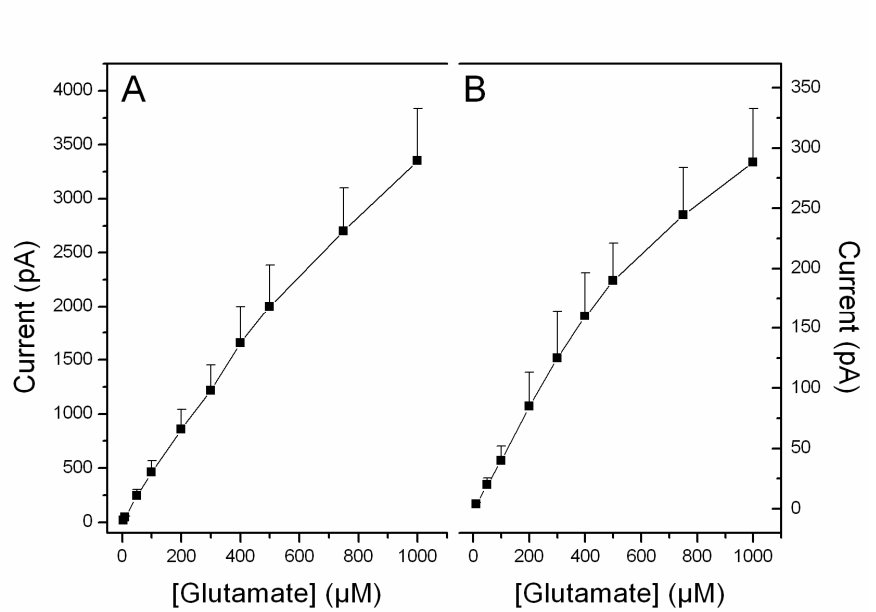

Figure 8: Linear range of the glutamate microsensor. ***A)*** *Response of the microsensor to different concentrations of glutamate in a FIA system at 1 ml/min (n = 8).* ***B)*** *Response of biofouled microsensors (post in vivo) to different concentrations of glutamate at oxygen deprived conditions (pO_2 ≈ 2%), in the presence of 200 µM AA and 50 µM UA (n = 6). Linearity was investigated with linear regression (p < 0.05; standardized residuals set at 2.0; not indicated).*

Performance of the microsensor in organotypic hippocampal slice cultures

Before evaluating the microsensor *in vivo*, its performance was studied in organotypic brain slice cultures (Fig. 9). Slice cultures mimic the living brain most closely, as they possess a three-dimensional organisation in which the different cell types are preserved (Bahr, 1995; Koeneman et al., 2004). In Fig. 9A it is shown that administration of saline did not induce a response. In Fig. 9B it was shown that the potent glutamate uptake inhibitor $_{DL}$-threo-β-benzyloxyaspartate ($_{DL}$-TBOA) increased the extracellular glutamate concentration approximately 3.5 fold (defined as the difference in current output between the glutamate and background microsensor after $_{DL}$-TBOA administration, divided by the difference prior to administration). As far as we know the influence of $_{DL}$-TBOA on extracellular glutamate levels in slice cultures

has not been studied before with a microsensor. Interestingly, patch-clamp recordings showed similar increases (Jabaudon et al., 1999). Next, the effect of high-K^+ was investigated (Fig. 9C). It is shown that within the first minute(s) after K^+-administration the glutamate levels increased approximately 4-fold. Interesting to note is the much faster response to high-K^+ compared to $_{DL}$-TBOA. A faster passive diffusion of K^+ over $_{DL}$-TBOA could be a possible explanation. However, results can also be explained by a delayed effect of the inhibitory action of $_{DL}$-TBOA, as glutamate and $_{DL}$-TBOA competitively interact with the membrane transporter, whereas high-K^+ induces an instantaneous depolarisation (Robert et al., 1997). These data illustrate that the fast response time of the microsensor is of advantage when investigating such dynamics.

It is concluded that the glutamate microsensor is a promising tool for detecting rapid changes of extracellular glutamate within brain slice cultures. It is of advantage that experimental conditions and implantation of the microsensor can be (visually)

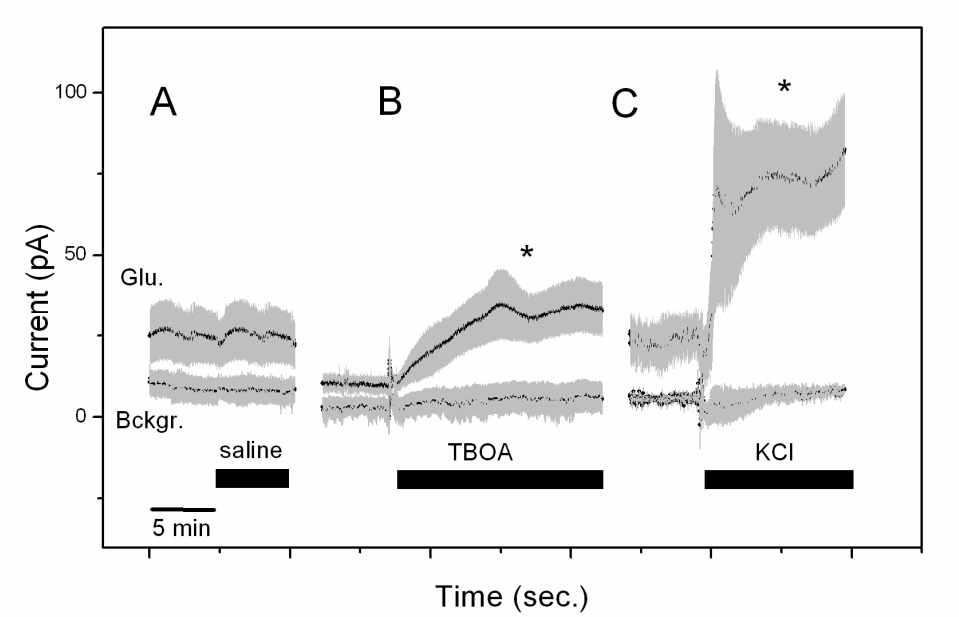

Figure 9: Performance of the microsensors in organotypic hippocampal slice cultures. Shown are the responses of the glutamate (Glu.) and background (Bckgr.) microsensors to bath application of ***A)*** *Saline (n=6),* ***B)*** *$_{DL}$-TBOA 100 µM (n=5) and* ***C)*** *KCl 100 mM (n=9). * Denotes a statistically significant difference (p < 0.05; One Way Anova followed by a Student-Newman-Keuls posthoc test).*

controlled and that experimental manipulations are easily accessible. In addition, brain slices contain much lower concentrations of reducing agents and relatively high oxygen levels are present (Brahma et al., 2000; Zimmer et al., 2000). The potential of the microsensor as an analytical tool *in vitro*, in acute hippocampal slices, is further explored in chapter 6.

Performance of the microsensor *in vivo*

Finally, the microsensor was evaluated *in vivo.* Three conditions were studied: the basal glutamate signal in the brain (Fig. 10A), the effect of $_{DL}$-TBOA (Fig. 10B) and the influence of euthanasia (Fig. 10C). First, the basal current output of the glutamate and background microsensor was investigated (Fig. 10A). The difference between both microsensors represented the extracellular glutamate concentration. A significant difference of 13 ± 2.9 pA (mean ± SEM; $p < 0.05$, M-W Rank Sum Test) was observed. From the previous paragraphs it is concluded that this current directly can be used for correlation to glutamate concentrations. As a result, this current corresponded to a glutamate concentration of 23.6 ± 5.3 µM, after recalculation with 0.55 ± 0.07 pA/µM (Fig. 9B). This value is in good accordance with previous observations by Kulagina et al., (1999) and with recent observations by Hascup et al., (2006), Nickell et al., (2006), Rutherford et al., (2006) and Stephens et al., (2006). However, (quantitative) microdialysis studies have reported basal glutamate concentrations in the range 1 to 5 µM (Miele et al., 1996). Therefore, the exact extracellular glutamate concentration is still a matter of debate. On one hand microdialysis might cause a significant underestimation of the glutamate levels, due to extensive brain damage induced by the probe (Khan and Michael, 2000), due to misinterpretation of the quantitative microdialysis data (Peters et al., 2000) or due to the composition of the dialysis perfusion medium (Lai et al., 2000; Rebec et al., 2005). On the other hand it is believed that microdialysis overestimates the glutamate levels, as the cellular high affinity uptake mechanisms are damaged (Cavalier et al., 2005). In this respect an overestimation of the detected glutamate levels by the microsensors can not be completely ruled out. In addition, it was observed that the basal glutamate levels were altered by the depth of anesthesia, i.e. the deeper the anesthesia the lower the glutamate levels (results not shown).

The effect of $_{DL}$-TBOA administration (1 mM; 500 nl injection) was shown in Fig. 10B. A significant increase of approximately 80% was observed, which

corresponded to an increase in glutamate of about 24 µM. Although the influence of $_{DL}$-TBOA on extracellular glutamate has not been investigated before with microsensors, the results were consistent with recently reported microdialysis studies (Baker et al., 2002; Xi et al., 2003).

The effect of euthanasia was shown in Fig. 10C. After administration of a chloralhydrate overdose, the microsensor output remained stable (not shown) and after a delay (up to 15 min) the response of both microsensors decreased significantly (Fig. 10C). This was an unexpected result as post mortem rises in extracellular glutamate were reported previously with microdialysis studies (Geddes et al., 1999). On the contrary, with euthanasia many processes occur, which makes the behaviour of the microsensor difficult to predict. Most likely the termination of breathing decreased the pO_2 levels and in turn limited the performance of the microsensor.

It is concluded that the microsensor is capable of detecting dynamic changes of extracellular glutamate *in vivo*. The potential of the microsensor as an analytical tool *in vivo* is further explored in chapter 7.

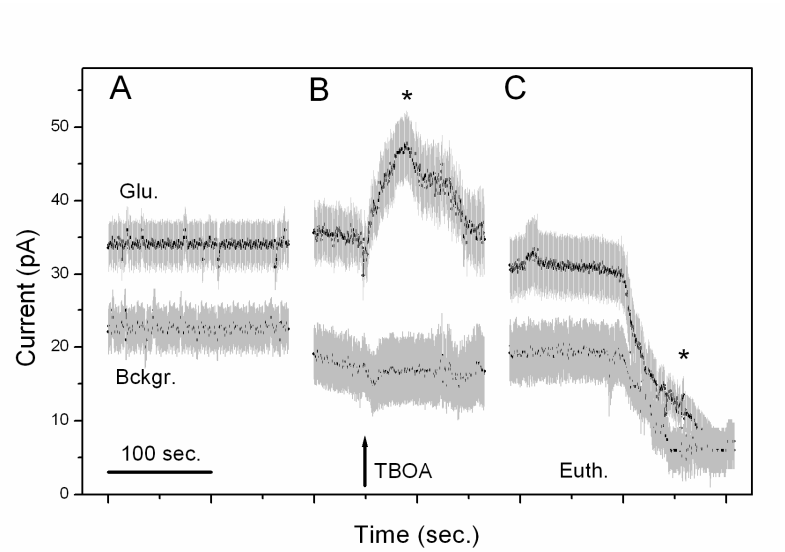

Figure 10: Performance of the microsensors in vivo. ***A)*** *Basal current output of the glutamate (Glu.; n = 37) and background microsensors (Bckgr; n = 29).* ***B)*** *Response of the microsensors to a micropipette infusion of $_{DL}$-TBOA (500 nl; 1 mM) (n = 5) and* ***C)*** *to euthanasia by a chloralhydrate overdose (n = 6; injection not indicated). * Denotes a statistically significant difference (p < 0.05; One Way Anova followed by a Student-Newman-Keuls posthoc test).*

5.4 Conclusion

A thorough characterization and evaluation of the glutamate microsensor is required before it can be applied as an analytical tool. The present evaluation of the hydrogel-coated glutamate microsensor indicated that several factors, which are encountered *in vivo* (but also *in vitro*), altered the performance of the microsensor significantly. The main disadvantage was the suppression of the response of the microsensor by reducing agents, in particular AA and UA. A positive aspect of this interference was that its mechanism was not linear, but virtually saturated at physiological concentrations. In addition, the response time of the microsensor improved drastically to approximately 8 seconds, and its response became independent on the type of calibration. For other interfering compounds, e.g. H_2O_2, the background microsensor could serve properly as a control sensor. Biofouling and oxygen deprivation also caused a decline in the response of the microsensor. Despite these limits, it is concluded that the microsensor is able to detect rapid changes of extracellular glutamate both *in vitro* (brain slice cultures) and *in vivo*. In chapter 6 and 7 the microsensor is applied on a routine base for both conditions.